EVALUATION OF 3D SURROGATE VEHICLES FOR AUTOMOTIVE SAFETY TESTS

William Buller
Michigan Technological University
United States

Niklas Lundin
AstaZero
Sweden

Kristian Karlsson
RISE Institutes of Sweden
Sweden

Daniel Aloi
Oakland University
United States

Paper Number 17-0023

ABSTRACT

This paper describes the development of evaluation methods to asses the suitability of a 3D surrogate vehicle for use in automotive safety tests for vehicles instrumented with radar. A vehicle with advanced driver assistance technology is tested in scenarios where it should take measures to avoid collisions. This is the Vehicle Under Test (VUT). In some scenarios, it is desired to see how the VUT performs in the presence of other vehicles. For safety reasons, the surrogate vehicle acts as the other vehicles in these situations. The term 3D surrogate vehicle is used to describe a surrogate suitable for tests from any approach direction. The 3D surrogate vehicle must satisfy three principal requirements:

1. The target must not cause injury or damage to test driver and vehicle.
2. The target must present a realistic response to advanced driver assist sensors and algorithms
3. The target should require minimal effort and time to re-construct following crash events.

The international community of automotive system and parts manufacturers, along with automotive safety assessment groups, is intent on accepting an initial 3D surrogate vehicle, referred to as the harmonized target, for testing advanced driver assistance systems. Measurements are being made by teams in the US and Sweden to compare the response of radar to the harmonized target along with real vehicles. This paper describes the rationale and theoretical foundation for these methods.

INTRODUCTION

For the accelerating development work ongoing in the active safety and autonomous functionality area it is vital that suitable surrogates are produced and accepted by the community. These surrogates are required, from early prototyping to rating tests, as crashable targets simulating real vehicles. Further, the surrogates have to be crashable with minor or no damage to the vehicle housing the functionality being tested. Different designs and concepts are possible, meeting e.g speed and maneuverability requirements for the specific test, but appearance to the relevant sensors and algorithms always has to be correct and consistent.

One vital factor for testing on proving grounds is a controlled and repeatable environment so that each VUT is subjected to the same test. This is the main differentiator, if safety is excluded, from testing in real traffic. The same traffic scenario has to be possible to repeat hundreds of times with an identical configuration to allow for validation of vehicle functionality. In these situations the surrogate vehicle has to maintain consistent properties for all relevant sensors, even if each test requires re-assembly of the surrogate. Here evaluation methods are a necessity since the human eye is not sufficient, all relevant spectrums and properties, such as radar cross section (RCS), have to be evaluated.

Knowledge of the statistics for energy returned from an object of interest (target) is typically the starting point for a radar system designer [1]. The RCS is a crucial element in understanding the ability of a radar to detect, track and identify the target. Early work to model target statistics and characterize the impact on radar performance were the subject of research by [2] and [3].

The procedures proposed here are practical measures of energy reflected by vehicles and surrogates in the plane of the targets during a full azimuth scan in a monostatic setup. The resulting 360 degree response enables characterization of the types of returns that can be expected by automotive radars. The procedures in this paper do not cover all aspects of the reflected energy, e.g., characterisation of the spatial distribution of the reflections on or within the target which are significant to the automotive radar response are needed to be characterised as well. This will be further elaborated in the "Discussion and Limitations" section.

METHODS AND DATA SOURCES

Measurements to characterize the full azimuth radar response of the 3D surrogate are collected following two separate methods:

1. This first method considers multiple vehicles and a surrogate measured in azimuth with the aid of an instrumented turntable at the at the Terrestrial Antenna Range, managed by the Applied EMAG and Wireless Lab, on the campus of Oakland University (OU) in Rochester, Michigan. Full azimuth scan of the targets were made at 28 and 94 GHz. These measurements are used to explore statistical approaches to evaluate the fidelity of a test surrogate.
2. Full azimuth scan of targets on open test area using a FMCW radar mounted on a movable trolley made by RISE Institutes of Sweden. This method positions a trolley via high precision GNSS (e.g. RTK-GPS) or a marked circle on the ground. Aiming accuracy of the radar towards the target is reduced compared to method 1, but on the upside this method is an alternative which can be implemented directly on the test-track without the need of a turn table.

Method 1: Measurements On Turntable

Sample Vehicles The team from Michigan Tech Research Institute and Oakland University collected radar measurements of the Guided Soft Target test system from Dynamics Research Incorporated and the four vehicles identified in Table 1.

Table 1: Vehicles and dimensions used for comparison in this study. Dimensions are shown in meters.

Make Model	Year	Length	Width	Height
Hyundai Accent	2008	4.05	1.70	1.47
Toyota Camry	2004	4.80	1.80	1.47
Ford Fiesta	2016	4.06	1.73	1.48
Subaru Impreza	2013	4.42	1.75	1.47
DRI GST	2016	4.02	1.71	1.43

Collection Geometry The collection system was set up 55 meters from the turntable platform. The entire system was contained within the back of a box truck to eliminate daily setup and any resulting system changes. The resulting spot size of the radar beam, full-width half maximum (FWHM), at the turntable was 1. 5 meter diameter. The center of this spot was 80 cm above the ground, as shown in Figure 1

.

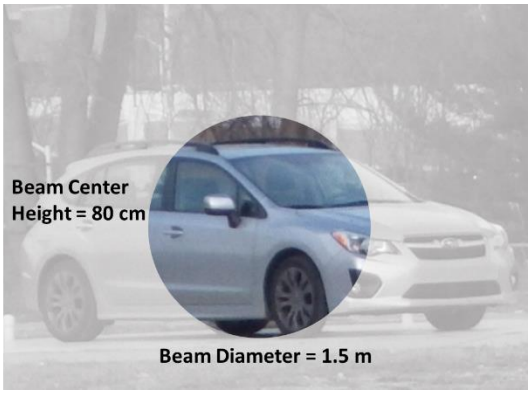

Figure 1: Overlay of beam foot- atop photograph of the Subaru.

Vehicles were positioned for measurement on the platform by placing the center of the vehicle at the center of the platform and facing the 0 degree rotation point, as in Figure 2.

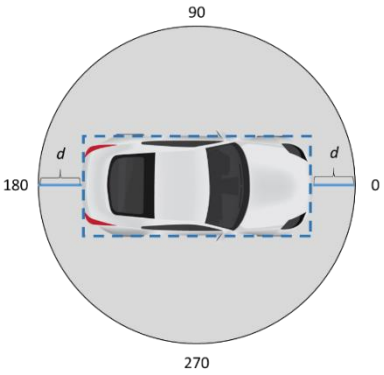

Figure 2: Measurements were collected with all targets set such that the center of the bounding box is at the center of rotation.

The target aspect angle convention is shown, with 0 degrees as the front of the vehicle and 180 degrees is the rear. The vehicle is centered when the body is aligned on the 0 degree axis and the distances, d, from front and rear to the edge of the turntable are equal.

Radar measurements and turntable angle measurements were made independently with GPS clocks and the data were aligned by linear interpolation. The received power is calibrated, via substitution [4].

Angular Sampling Radar measurements were collected while the turntable was rotated at a rate suitable to oversample the angular bandwidth of the targets. The collection system makes a single frequency measurement 14.3 times per second. A full representation of the backscattering fields (and therefore RCS) of an object from field samples is dependent on the wavelength and geometry of the collection [5] and [6].

Assuming the maximum scene dimension, ρ_{max}, shown in (Equation 1) is limited by the null-to-null beam-width of our antennas (2.6°),

$$\rho_{max} = 2\,R\tan(\beta_{null}/2) \qquad \text{(Equation 1)}$$

where R is the range from radar to the target, the angular sampling requirement (maximum interval in angular measurements needed) to reconstruct the EM field is given by (Equation 2) [5].

$$\Delta\phi_{max} = \frac{\lambda_0\sqrt{R^2 + (\rho_{max})^2}}{4R\rho_{max}} \qquad \text{(Equation 2)}$$

The theoretical angular sampling requirements are tabulated in Table 2. The measured data is confirmed to be oversampled by inspecting the Fourier transform of the azimuth data and observing that the azimuth sampling is band-limited.

Table 2 – Theoretical azimuth sampling requirement by radar band (wavelength) mapped into the turnatable parameters of the facility to estimate samples required and collection time.

Parameter	28 GHz	94 GHz
wavelength, λ	0.01	0.00
range, R	55.00	55.00
beam width, ρ_{Max}	2.50	2.50
angular interval, $\Delta\varphi$	0.06	0.02
sampling rate, f_S	14.00	14.00
angular rate, $\Delta\varphi_S$	0.88	0.24
collection time in minutes	6.78	24.87
# samples	5697	20891

Measurements Calibrated radar returns from one of the vehicles and the GST are plotted in Figure 3 at 28 GHz and 94 GHz. The strong specular return of the Ford Fiesta at 90 and 270 degrees in aspect (side view) are accompanied by low measurement returns at oblique angles away from the front, side and rear.

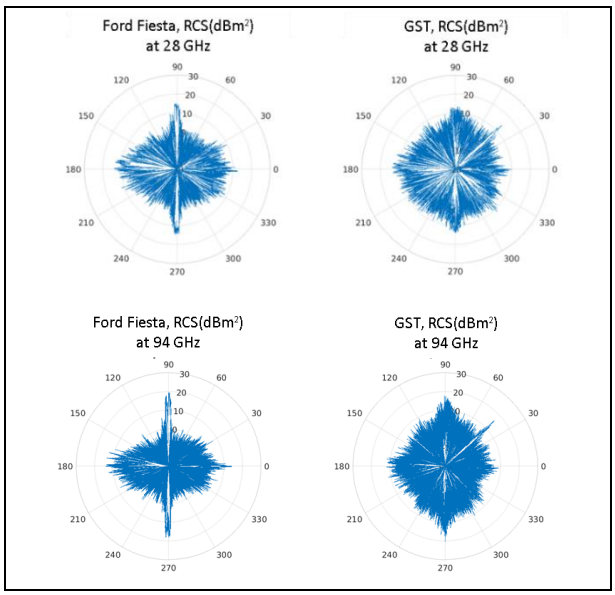

Figure 3: Polar plots of radar returns a Ford Fiesta and Subaru the GST, measured at 28 GHz (top) and 94 GHz (bottom).

The same is observed for all of the vehicles, and is expected for radar targets with smooth, flat sides. However, the GST is a soft target and this feature is less pronounced.

Method 2: Measurements At Test Track

Sample Vehicle The research project HiFi Radar Target (with participants from RISE, AstaZero, Volvo Cars and Autoliv) collected radar measurements of a Volvo S60, as described in Table 3

Table 3: Vehicle and dimensions used. Dimensions are shown in meters.

Make Model	Year	Length	Width	Height
Volvo S60	2015	4.63	2.10	1.48

Collection Geometry This method enables data collection on a test-track and does not require a turntable for rotation of the target (vehicle or surrogate). Here an azimuthal scan is performed by parking the vehicle on a fixed spot on a large flat asphalt plane (High Speed Area at AstaZero [7]) and move the measurement equipment around the target during data collection. For collecting RCS samples a W-band FMCW modulated radar with a bandwidth of 1 GHz centered around 76.5 GHz was used. This radar had a waveguide output which was connected to a lens horn antenna with a beam width of 2.5°. For precise movement the measurement equipment was mounted on a trolley which was manually moved along a circle marked on the ground and the vehicle was positioned in the center of the circle according to Figure 4. It is also possible to use a high precision GNSS receiver (e.g. RTK-GPS) and a robot to automatically position the trolley. The radar was mounted on the trolley so that it was always facing the center of the circle. The radius of the circle was for this measurement set to 18 meters. At this distance the diameter of resulting spot size (defined by the 3 dB beam width) of the radar at the center point was 0.79 m in diameter.

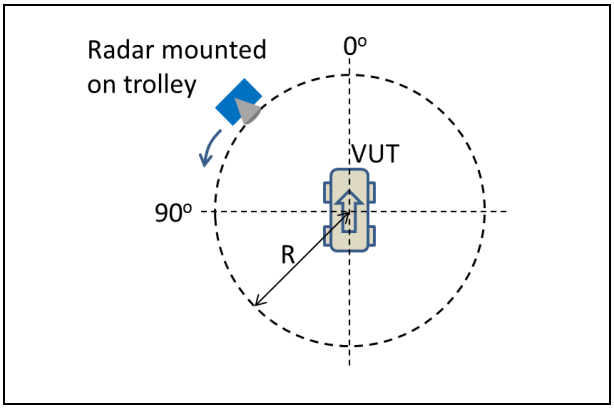

Figure 4: Description of the measurement setup. Radius R = 18 m.

Calibration To evaluate the system, the RCS of a sphere was measured. As a theoretical sphere has constant monostatic RCS independent of angle the measured response should ideally be constant and is therefore a good candidate for basic estimation of the uncertainty of the method. Major factors that influence accuracy are imperfections in positioning and aiming abilities, accuracy of the radar, influence of ground reflection and a non-perfect target (i.e. the sphere). In Figure 5, the measured RCS as function of angle of the sphere is presented. The sphere had a radius of 125 mm and the standard deviation of the collected data was 0.9 dB.

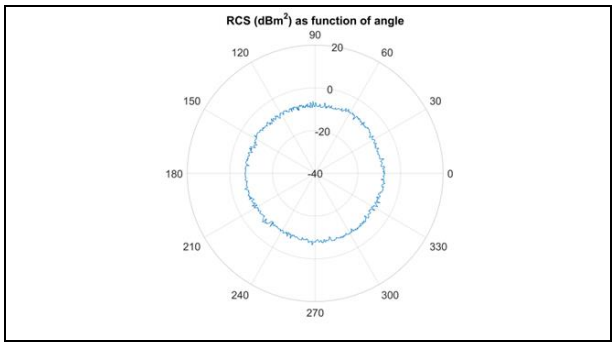

Figure 5: Evaluation of the measurement system: RCS of the sphere as function of angle.

Measurements Returns of the vehicle at two different heights are plotted in Figure 6. By comparing the measurement at 0.6 m height with the measurement at 1.1 m height it can be seen that RCS is lower at 1.1 m (due to less car body and more windows at that 1.1 m height compared to 0.6 m height). This is especially evident in the front direction.

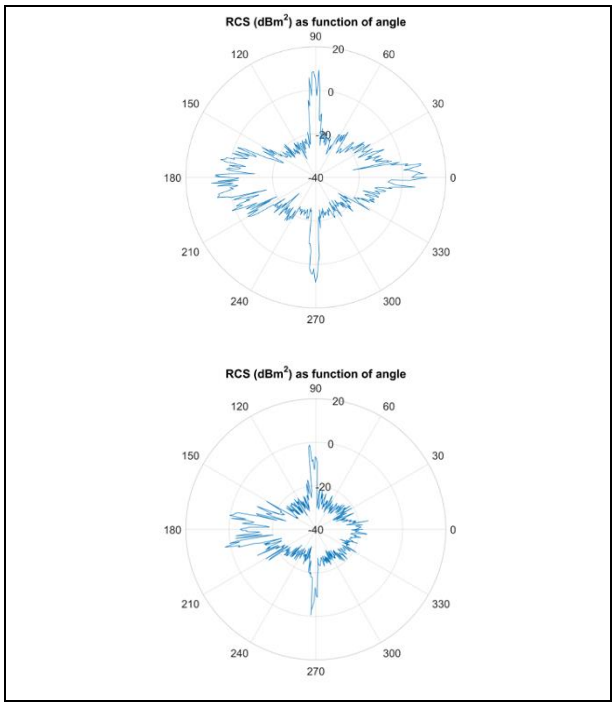

Figure 6: Polar plots of radar returns from the Volvo S60 vehicle. The orientation of the vehicles is the nose is at 0 degrees, so that the vehicle would be aimed to the right in the plot above. Measurements at radar height 0.6 m (top), and 1.1 m (bottom).

RESULTS

The results of this research are the development of an evaluation strategy for surrogate vehicles and demonstration that a reasonable protocol can be developed to make such an evaluation at test tracks. The azimuthal scans of the vehicles and GST can be used to sample ensembles of radar returns for a set of viewing aspect angles. For an ensemble of aspect angles, we can generate the empirical cumulative density function (CDF) of the radar reflections. The CDF provides a direct measure of the target's role in the performance of a threshold detector. At a given value of RCS on the independent axis, the CDF, see example in Figure 7, relates the ratio of measurements that fall below that value. Measurements below the threshold confirm a null-hypothesis, $H0$, in the presence of the sample, $H1$. The probability of this happening, $P(H0|H1)$, is the type 2 error rate or probability of missed detection.

The maximum separation between a pair of CDFs is the definition of the Kolmogorov-Smirnov two sample test statistic, $\gamma_{KS,2}$ [8]. Therefore, these measurements offer a path to develop a hypothesis test for target evaluation.

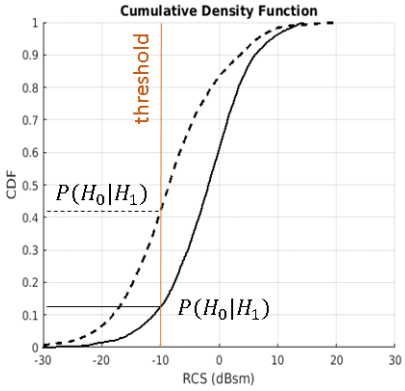

Figure 7: An example cumulative density function with a threshold and the type 2 error rates for the two samples shown by dashed and solid CDF curves.

Method 1: Turntable Results

Example results were generated for three windows of aspect in Table 4. The CDFs show that, in general, the GST is more detectable than the vehicles used for comparison. This is especially true at nose aspects. The CDF plots for the measurements at 28 GHz and 94 GHz are shown in Figure 8, 9, and 10, for the aspect windows.

The CDFs show that the GST is likely to underestimate the type 2 errors that would be expected using real vehicles (it will provide optimistic performance results).

Table 4: Aspect angles in each of the windows used for statistical analysis.

Aspect Window	Aspect Angles in Window
Nose	{-45, ... 45}
Side	{45, ... 135} and {225, ... 315}
Tail	{135, ... 225}

The GST does not reflect power, however, at levels that are inconsistent with returns of vehicles. So it is not producing reflections at levels higher than the vehicles, it is simply not producing as many low returns. Thus, from the turntable analysis, a radar intended to detect vehicles should perform well against the GST.

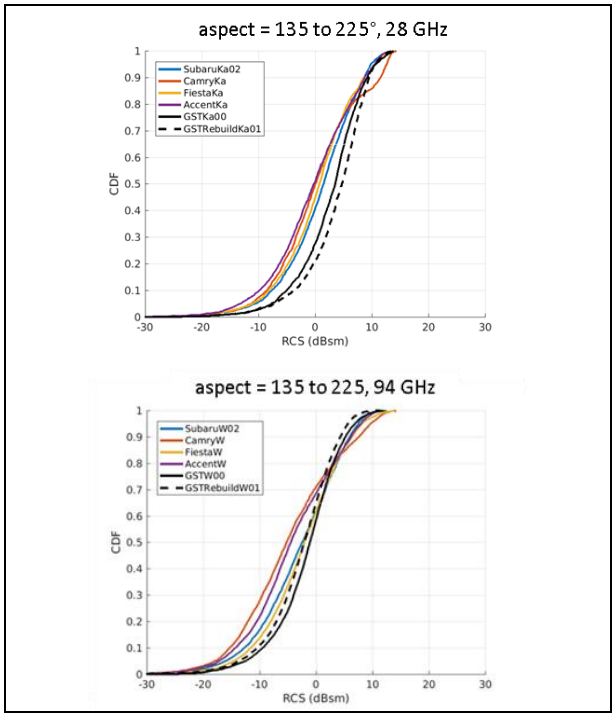

Figure 8: The CDFs of the measurements at tail aspects at 28 GHz at top, and 94 GHz at bottom.

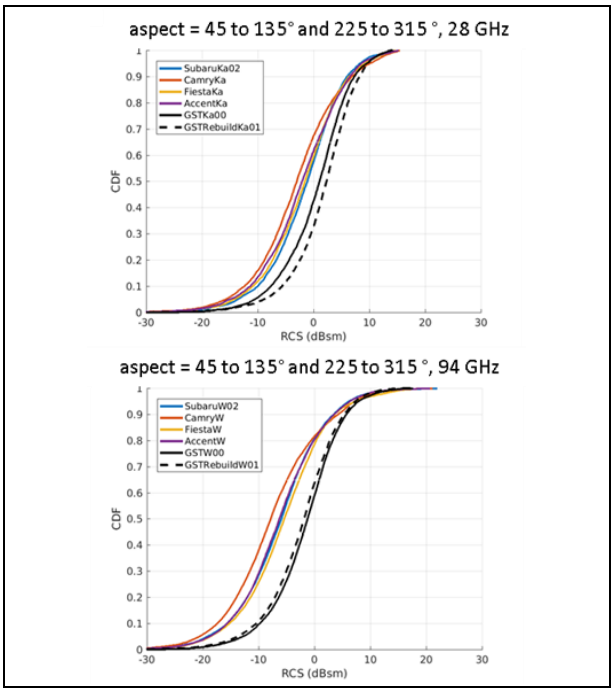

Figure 9: The CDFs of the measurements at side aspects at 28 GHz at top, and 94 GHz at bottom.

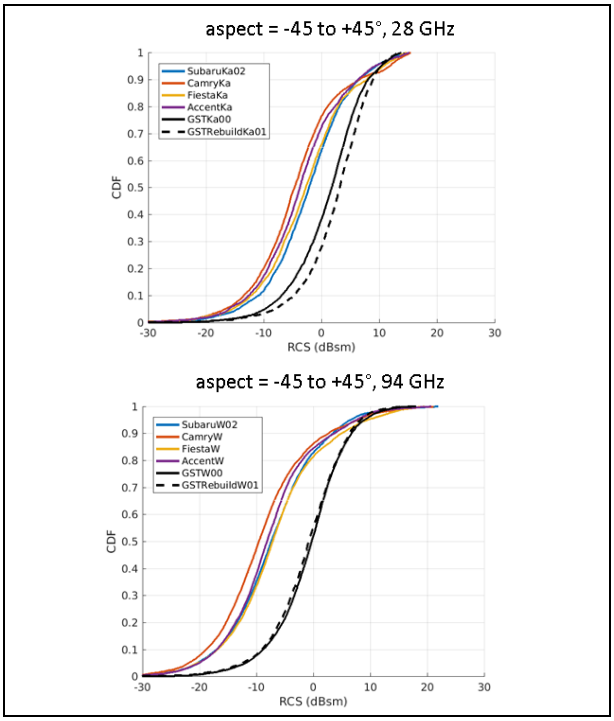

Figure 10: The CDFs of the measurements at nose aspects at 28 GHz at top, and 94 GHz at bottom.

Examples of the value of $\gamma_{Ks,2}$ are shown for pairs of targets in Table 5

Table 5: Example values of $\gamma_{KS,2}$ for pairs of targets, including vehicles and surrogate using at 28 GHz, and aspects of 135…225°.

	Toyota Camry	Ford Fiesta	Hyundai Accent	GST
Subaru Impreza	0.097	0.059	0.116	0.148
Toyota Camry		0.083	0.086	0.228
Ford Fiesta			0.090	0.196
Hyundai Accent				0.242

A threshold can be developed based on the values based on vehicles only and used to evaluate the surrogate. The development of a threshold is beyond the scope of this paper. However, the values in , show that the values comparing the GST and the vehicle (the last column, in grey) are all greater than the values comparing vehicles. While this approach provides a definitive evaluation, it requires a statistically rich data set and definition of the confidence interval.

Method 2: Test Track Results

The amount of captured data was not enough to create CDFs of the measurements in the three aspect windows defined in method 1. Therefore a CDF from 0 to 360 degrees is plotted for the two measured heights.

The CDFs, in Figure 11, show that, in general, measurements at 1.1 m height reflects less power compared to measurements at 0.6 m height. This is, as previously stated, probably due to less car body and more windows at that 1.1 m height compared to 0.6 m height.

DISCUSSION AND LIMITATIONS

Measurements of vehicles and a soft surrogate were made under different conditions in Sweden and the US. The radar returns show a similarity in domain, mostly between -20 to 20 dBsm. The angular responses show similar features, with the vehicles producing pronounced specular returns at the sides and more complicated structure near front and rear. The measurements in US are used to demonstrate a method for evaluating the power distribution of a soft surrogate to induce similar errors in a collision avoidance system via the cumulative density function. The measurements in Sweden support the development of protocols that can be used at safety test tracks, allowing for tests that ensure each VUT is subjected to similar test conditions.

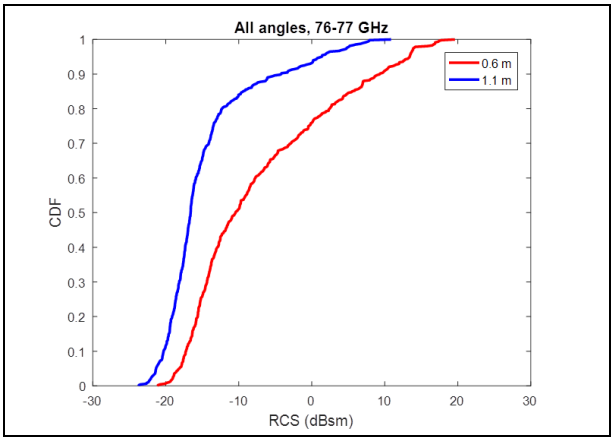

Figure 11: The CDF for two measurement heights of the target is plotted.

The research detailed in this paper is intended to provide input to ISO work on 3D target specification, as well as facilitating the work on the harmonized 3D target. These measurements are calibrated, but are not intended as far-field target RCS measurements.

The spatial distribution on the target of the reflected energy is not covered by these methods, and therefore complementary characterizations and measures are needed, possibly both in range and for viewing angle. Finally close range characterisation of the target (which is directly dependent on its spatial distribution) is necessary for automotive functions operating at close range.

CONCLUSIONS AND RELEVANCE TO SESSION SUBMITTED

Methods to evaluate surrogate vehicles for automotive safety tests need to be defined. The research here develops an initial approach to evaluate surrogate vehicles at test tracks. This requires that measurements have a well defined protocol and decision test. Our results suggest that a protocol using the cumulative density function of measurements over a defined set of aspect angles provides a basis for comparing surrogates with a pool of representative objects. Further, the results suggest that this approach can be practiced at test tracks.

The use of the Kolmogorov-Smirnov two sample test statistic provides a metric that to evaluate surrogates with an hypothesis test. However, the results also high-light the need for a statistically rich set of

measurements to support this approach, along with further development of the theoretical framework for computing the confidence of such a test.

ACKNOWLEDGEMENTS

This work has partly been financed by: The Swedish government agency for innovation systems (VINNOVA) within the HiFi Radar Target project, and used data collected during the Comparison of RADAR returns from vehicles and Guided Soft Target (GST) project funded by the US Department of Transportation's National Highway Transportation Safety Administration.

The authors would like to thank Henrik Toss and Urban Lundgren at RISE Institutes of Sweden for valuable work during the field tests that are presented in this paper. The measurements at Oakland University were made possible with the contributions of Brian Wilson, Benjamin Hart, and Sam Aden of MTRI, Garrick Forkenbrock of NHTSA, Ian Davis of TRC, and Ahmad Yacoub, and Ahmad Salih of Oakland University.

REFERENCES

1. Kulemin, Gennadiĭ Petrovich. Millimeter-wave radar targets and clutter. Artech House, 2003.
2. Marcum, J. I. A statistical theory of target detection by pulsed radar. No. RM-754. RAND CORP SANTA MONICA CA, 1947.
3. Swerling, P. Probability of Detection for Fluctuating Targets, RM-1217, RAND CORP SANTA MONICA CA, 1954.
4. Knott, Eugene F. *Radar cross section measurements*. Springer Science & Business Media, 2012.
5. Bucci, O., & Franceschetti, G. On the spatial bandwidth of scattered fields. IEEE Transactions on Antennas and Propagation, 35(12), 1445–1455, 1987.
6. Buddendick, H., & Eibert, T. F. Acceleration of Ray-Based Radar Cross Section Predictions Using Monostatic-Bistatic Equivalence. IEEE Transactions on Antennas and Propagation, 58(2), 531–539, 2010.
7. http://www.astazero.com/the-test-site/test-environments/high-speed-area/
8. Olofsson, P. *Probability, Statistics, and Stochastic Processes*. New York, John Wiley & Sons, Inc. 2012.